Lower limit on the ultrahigh-energy proton-to-helium ratio from the measurements of the tail of the X_{max} distribution

Ivan S. Karpikov,[1] Grigory I. Rubtsov,[1] and Yana V. Zhezher[1,2,*]

[1]*Institute for Nuclear Research of the Russian Academy of Sciences, 117312 Moscow, Russia*
[2]*Faculty of Physics, M.V. Lomonosov Moscow State University, 119991 Moscow, Russia*

(Received 10 May 2018; revised manuscript received 19 September 2018; published 5 November 2018)

There are multiple techniques to determine the chemical composition of the ultrahigh-energy cosmic rays. While most of the methods are primarily sensitive to the average atomic mass, it is challenging to discriminate between the two lightest elements: proton and helium. In this paper, the proton-to-helium ratio in the energy range $10^{18.0}$ eV to $10^{19.3}$ eV is estimated using the tail of the distribution of the depth of the shower maximum X_{max}. Using the exponential decay scale Λ measured by the Pierre Auger Observatory and the Telescope Array experiment we derive the 68% CL constraints on the proton-to-helium ratio $\mathrm{p/He} > 7.3$ and $\mathrm{p/He} > 0.43$ for $10^{18.0} < E < 10^{18.5}$ eV and $10^{18.3} < E < 10^{19.3}$ eV correspondingly. It is shown that the result is conservative with respect to the admixture of heavier elements. We evaluate the impact of the hadronic interaction model uncertainty. The implications for the astrophysical models of the origin of cosmic rays and the safety of the future colliders are discussed.

DOI: 10.1103/PhysRevD.98.103002

I. INTRODUCTION

The mass composition of the ultrahigh-energy cosmic rays lies among the key tasks of major present-day and upcoming experiments. The precise knowledge of the composition is important for understanding the cosmic-ray production mechanism in the sources and its population [1]. Moreover, composition at the highest energies is the decisive factor for the observable flux of cosmogenic photons [2,3] and neutrinos [4,5], see [6] for a review. The photons and neutrinos are more efficiently produced by the primary protons compared to heavier elements due to the highest energy per nucleon. The diversity of the models may be illustrated with the two antipodal examples namely the dip model [7–9] and the disappointing model [10]. The dip model has purely proton composition and as a consequence predicts observable fluxes of the cosmogenic photons and neutrino. The model is named after the dip spectral feature which is naturally explained with the electron-positron pair production by protons. The disappointing model includes both protons and nuclei in the source and assumes that the acceleration of primary nuclei in the sources is rigidity-dependent with relatively low maximum energy of acceleration. It was named "disappointing," because in this case there are no pion photo-production on CMB in extragalactic space and consequently no high-energy cosmogenic neutrino fluxes. Disappointing model predicts no GZK-cutoff [11,12] in the spectrum and shows no correlation with nearby sources due to deflection of the nuclei in the galactic magnetic fields up to the highest energies.

Another implication of the mass composition at ultrahigh energies is the investigation of safety of the future colliders. In certain theoretical models characterized by additional spatial dimensions, the production of nonevaporating microscopic black holes becomes possible. This phenomenon was taken into consideration in the framework of the Large Hadron Collider (LHC) safety analysis [13,14]. The proof of the LHC safety is based on the constraints on the black hole production derived from the stability of dense astrophysical objects, such as white dwarfs and neutron stars. The latter interact with the ultrahigh-energy cosmic rays with the center of mass energies larger than ones achieved at LHC. One may ascertain the safety of the future 100 TeV colliders by studying the interaction of the cosmic rays of the highest energies. The primary protons again play an important role as the production of the black holes is determined by the energy per nucleon. It was shown that the charged stable microscopic black hole production may be excluded already, while the exclusion of the neutral black holes would require a precise knowledge of the proton fraction at the ultrahigh energy [15].

One of the most common approaches is the measurement of the longitudinal shape of the extensive air showers (EAS). The depth of a shower maximum, or X_{max}, is used as a composition-sensitive variable [16]. The measurements of the mean X_{max} gives the estimate of the average atomic mass, while the study of the X_{max} distribution and its moments may resolve the multicomponent composition, see [17–19].

*zhezher.yana@physics.msu.ru

Composition studies with the use of $X_{\max}$ measurements were performed by both the Pierre Auger Observatory [20] and the Telescope Array [21,22]. Besides the derivation of the average atomic mass of primary particles, the data on the full shape of $X_{\max}$ distribution may be used to determine the possible fluxes of primary nuclei. This is performed by comparison of the experimental data with Monte-Carlo simulated sets.

The Pierre Auger Observatory data set is comprised of nearly 11-year data collected by the Fluorescence detector and the 5-year data collected with the High Elevation Auger Telescopes (HEAT) which extend the field of view of the Coihueco telescope station. The experimental data are fit jointly with the mixture of the proton, helium, nitrogen, and iron Monte-Carlo sets thus allowing to obtain the mass fraction of the corresponding nuclei. The best fit imply that non-zero helium flux is expected in the energy range $10^{17.2}$–$10^{17.7}$ eV and $10^{18.4}$–$10^{19.5}$ eV, while for the range $10^{17.7}$–$10^{18.4}$ eV it is compatible with zero at 2σ confidence level. An improved fitting procedure for the Pierre Auger Data was proposed to reduce the effects of hadronic models uncertainties [23]. This result shows an indication of the presence of helium nuclei in the observed UHECR flux in the same energy band at somewhat higher significance.

In case of the Telescope Array, 8.5-year data from the Black Rock Mesa and Long Ridge fluorescence detectors operating in hybrid mode together with the surface detectors is used. It was shown that pure protonic composition is expected in the energy range $10^{18.25}$–$10^{19.10}$ eV at the 95% confidence level. However, for higher energies the admixture of heavier elements cannot be excluded.

The tail of the $X_{\max}$ distribution may be studied independently of the main part of the distribution. It may be fit with an exponential function $\exp(-X_{\max}/\Lambda)$, where Λ is called the attenuation length. The attenuation length is found to be sensitive to the proton-air interaction cross section. The first results by this method were obtained by the Fly's Eye Collaboration [24,25] followed by the results of the Pierre Auger and Telescope Array Collaborations [26–28]. It was shown in [29] that the attenuation length may be used to estimate the proton-to-helium ratio p/He. The latter estimate has only minor dependence on the hadronic interaction models and $X_{\max}$ experimental systematic uncertainties.

The proton-to-helium ratio is directly measured below the knee and it allows to constrain different astrophysical models of the origin of cosmic rays [30,31]. The measurements of the proton-to-helium ratio at the ultrahigh energies may be used similarly to discriminate between different source models. As a recent example, a modified dip model [32] confirms the measured spectrum of the ultrahigh-energy cosmic rays for the value of proton-to-helium ratio p/He = 5. Furthermore, the value of p/He used jointly with the other composition studies will allow to pinpoint the flux of the primary protons. The latter is an important quantity as discussed above.

The present work is dedicated to the determination of proton-to-helium ratio of ultrahigh-energy cosmic rays in the energy range from $10^{18.0}$ eV to $10^{19.3}$ eV based on Pierre Auger Observatory and on the Telescope Array measurements of the attenuation length [26–28]. The data are compared to the Monte-Carlo simulations using the CORSIKA (version 7.6400) package [33] along with the QGSJET II-04 [34,35] and EPOS-LHC [36] hadronic interaction models.

The paper is organized as follows. In Sec. II the analysis method is explained along with Monte-Carlo simulations. The results on proton-to-helium ratio are presented in Sec. III. Section IV contains concluding remarks.

II. METHOD AND MONTE-CARLO SIMULATIONS

The method generally follows the work of Yushkov *et al.* [29] to derive the proton-to-helium ratio using the measurements of the attenuation length by the Pierre Auger Observatory [27] and the Telescope Array collaboration [26].

At first, the simulated sets of extensive air showers initiated by primary protons, helium and carbon are produced with the use of the CORSIKA package [33]. Simulations are performed separately with QGSJET II-04 [35] and EPOS-LHC [36] hadronic interaction models for both experiments. In Auger case, for the energy range $10^{18.0}$ eV $< E < 10^{18.5}$ eV with spectral index -3.293 [37] 17 098 events are simulated with EPOS-LHC model, and 20 913 events are simulated with QGSJET II-04 model. For the Telescope Array, 17 354 events are simulated for both hadronic interaction models for each species in the energy range from $10^{18.3}$ eV to $10^{19.3}$ eV with the spectrum obtained by the Telescope Array collaboration defined by the spectral index -3.226 for $E < 10^{18.72}$ eV and -2.66 for $E > 10^{18.72}$ eV [38].

At the second step, the simulated sets are "mixed" in different proportions from p/He = 0.01 to p/He = 100.0. For each mixture the $X_{\max}$ distribution slope is fit exponentially to derive the attenuation length for a mixed composition model.

An important constituent of this method is the choice of the starting point of the fit: it can be defined in many different ways. In the initial papers [24,25] the lower range of $X_{\max}$ fit was fixed at the constant values $X_{\max} = 760\,\mathrm{g/cm^2}$ and $X_{\max} = 830\,\mathrm{g/cm^2}$, respectively. Yushkov *et al.* [29] have proposed another determination of lower fit range, which involves carbon $X_{\max}$ distribution: the lower limit is defined as a value at which only ≈0.5% of the carbon-initiated showers get into the fitting range. In the present paper, the Pierre Auger instance is treated according to [28]. Experimental data analysis involves a three-step procedure, where first of all $X_{\max}$-interval containing

99.8% of most central events is found. Then the derived distribution is used to obtain $X_{\max}$-intervals containing 20% of most deeply penetrating showers. Finally, upper end of the fit range is chosen to exclude 0.1% of all events. This approach results in the following $X_{\max}$ fit range which is implemented in the present work: $X_{\max,\mathrm{start}} = 782.4$ g/cm^2 to $X_{\max,\mathrm{end}} = 1030.1$ g/cm^2 for the $10^{18.0}$–$10^{18.5}$ eV.

For the Telescope Array case we follow the method implemented by Abbasi *et al.* [26], where the lower limit is defined as the $X_i = \langle X_{\max}\rangle + 40$ g/cm^2, where $\langle X_{\max}\rangle$ is the average value of a given distribution.

Finally, after performing the fit of each mixture's $X_{\max}$ distribution, Λ_i values are obtained as a function of p/He ratio. The constraints on the proton-to-helium ration are then obtained by comparing these values with the experimental Λ values [26–28]. The lower limit on the proton to helium ratio at 68% CL corresponds to the lower limit of the experimentally measured Λ value is derived with the use of measured experimental uncertainties.

III. RESULTS

We present the $X_{\max}$ distributions and corresponding fits of exponential tails for proton, helium, and carbon Monte-Carlo simulated sets in Figs. 1 and 2.

Λ as a function of proton-to-helium ratio in QGSJET II-04 and EPOS-LHC models is shown in Figs. 3 and 4 with a black line. The plot includes the proton-to-helium ratio range from p/He = 0.01 to p/He = 100 with a step $\log_{10}\Delta = 0.2$.

For the Auger case, experimental value of $\Lambda = 57.4 \pm 1.8_{\mathrm{stat}} \pm 1.6_{\mathrm{syst}}$ g/cm^2 [28] in the energy range $10^{18.0}$ eV $< E < 10^{18.5}$ eV. This results in the following limits:

$$\begin{aligned} &\mathrm{p/He} > 7.3\,(68\%\ \mathrm{CL}) \quad \mathrm{QGSJET\,II\text{-}04},\\ &\mathrm{p/He} > 24.0\,(68\%\ \mathrm{CL}) \quad \mathrm{EPOS\text{-}LHC}. \end{aligned} \tag{1}$$

The TA data provides an independent measurement of the Λ and corresponding constraints on the proton-to-helium ratio. Comparing the Monte-Carlo function with the experimental value $\Lambda = 50.47 \pm 6.26$ g/cm^2 obtained by the Telescope Array collaboration [26] in the energy range $10^{18.3}$ eV $< E < 10^{19.3}$ eV we arrive at the following lower limits on the proton-to-helium ratio:

$$\begin{aligned} &\mathrm{p/He} > 0.43\,(68\%\ \mathrm{CL}) \quad \mathrm{QGSJET\,II\text{-}04},\\ &\mathrm{p/He} > 0.63\,(68\%\ \mathrm{CL}) \quad \mathrm{EPOS\text{-}LHC}. \end{aligned} \tag{2}$$

We note that the pure proton composition is well compatible with the measured attenuation length.

The stability of the method in respect to the admixture of the heavier elements is studied. For this reason, the analysis is repeated for three-component mixtures containing 25%, 50%, and 75% of carbon and corresponding Λ is shown in Figs. 3 and 4 by the blue, red, and yellow lines, respectively. One may see that the constraints (1) and (2) are conservative to addition of the heavier elements as expected in [29].

One may further study the three-component mixture of protons, helium and carbon. By calculating Λ for all possible combinations we arrive to the following lower limits on the fraction of protons in the three-component mixture for the Pierre Auger Observatory:

$$\begin{aligned} &\mathrm{p/(p+He+C)} > 0.8\,(68\%\ \mathrm{CL}) \quad \mathrm{QGSJET\,II\text{-}04},\\ &\mathrm{p/(p+He+C)} > 0.96\,(68\%\ \mathrm{CL}) \quad \mathrm{EPOS\text{-}LHC}. \end{aligned} \tag{3}$$

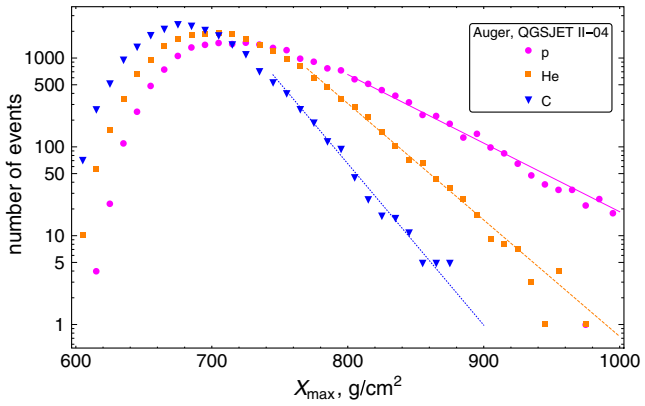

FIG. 1. $X_{\max}$ distributions for $10^{18.0}$ eV $< E < 10^{18.5}$ eV for the Pierre Auger Observatory for proton (magenta), helium (orange), and carbon (blue) Monte-Carlo distributions simulated with QGSJET II-04. $X_{\max}$ distribution's tail exponential fit $\exp(-X_{\max}/\Lambda)$ is shown for each Monte-Carlo with a line of the corresponding color.

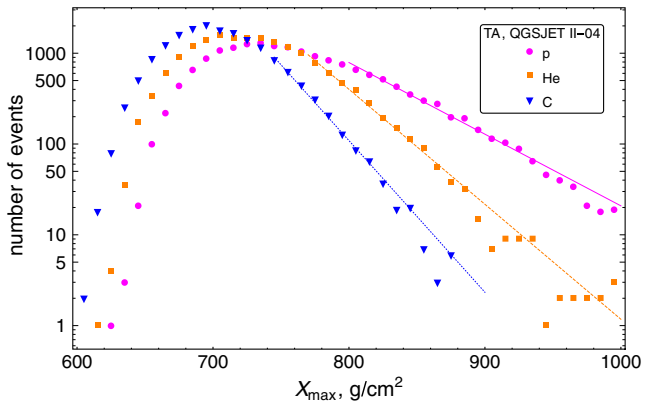

FIG. 2. $X_{\max}$ distributions for $10^{18.3}$ eV $< E < 10^{19.3}$ eV for the Telescope Array for proton (magenta), helium (orange), and carbon (blue) Monte-Carlo distributions simulated with QGSJET II-04. $X_{\max}$ distribution's tail exponential fit $\exp(-X_{\max}/\Lambda)$ is shown for each Monte-Carlo with a line of the corresponding color.

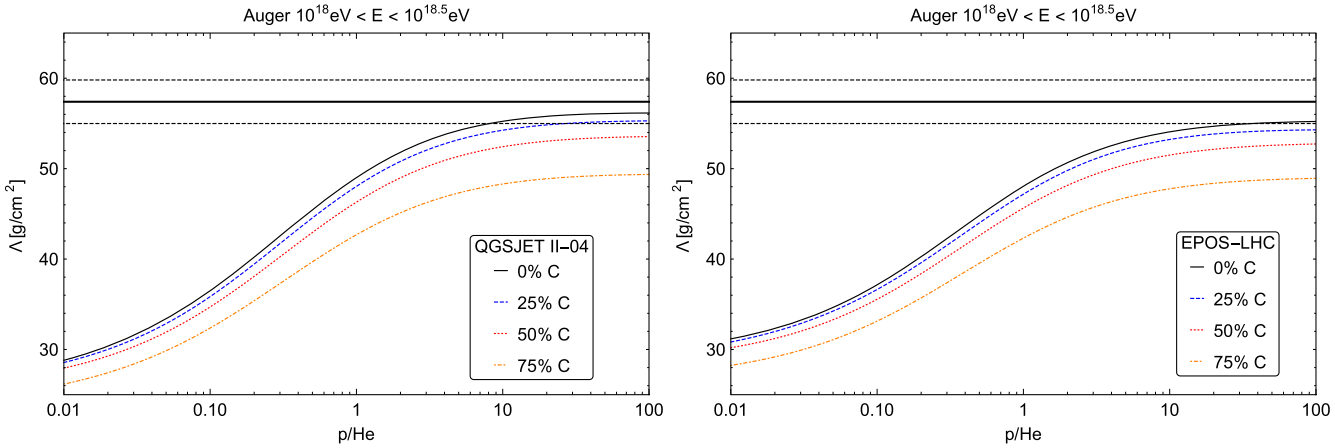

FIG. 3. Λ parameter as a function of proton-to-helium ratio for $10^{18.0}$ eV $< E < 10^{18.5}$ eV for two-component mixture (p and He, black line) and three component mixtures (p, He and 25% C—green line; p, He and 50% C—red line; p, He and 75% C—orange line) of Monte-Carlo events simulated with QGSJET II-04 (left) and EPOS-LHC (right). Black solid and dashed lines correspond to the experimental value $\Lambda = 57.4 \pm 1.8_{\rm stat} \pm 1.6_{\rm syst}$ g/cm^2 obtained by the Pierre Auger Observatory [28].

And for the Telescope Array:

$$\begin{aligned} &{\rm p}/({\rm p}+{\rm He}+{\rm C}) > 0.20\,(68\%\ {\rm CL}) \quad {\rm QGSJET\,II\text{-}04},\\ &{\rm p}/({\rm p}+{\rm He}+{\rm C}) > 0.23\,(68\%\ {\rm CL}) \quad {\rm EPOS\text{-}LHC}. \end{aligned} \tag{4}$$

Derived constraints are compatible with the predictions for proton flux based on $X_{\rm max}$ measurements by both the Pierre Auger Observatory and the Telescope Array [20–22]. Due to smaller experimental uncertainties, the proton-to-helium ratio is derived more precisely with the Auger data.

The discussion of the possible instrumental effects is in order. The $X_{\rm max}$-distributions are known to be affected by the geometrical acceptance of the detectors as well as the reconstruction procedure, while in the scope of this paper Λ values were derived for both TA and Auger assuming that protons, helium, and carbon nuclei are registered with the same efficiency. In the Auger case, the unbiased $X_{\rm max}$-distribution is guaranteed by applying the fiducial cuts which extract 20% of the most deeply penetrating showers and the events which have geometries allowing the complete observations of $X_{\rm max}$ values in the derived range [27]. For the TA, it was shown in [26], that there is no bias introduced to the Λ value if either the thrown proton distribution without any detector effects is used, or the one which was propagated through the detector and then reconstructed. Moreover, as it is shown in [39], the precision of the $X_{\rm max}$ reconstruction for iron Monte-Carlo events is somewhat higher than the one for proton events. No biases are expected for intermediate nuclei

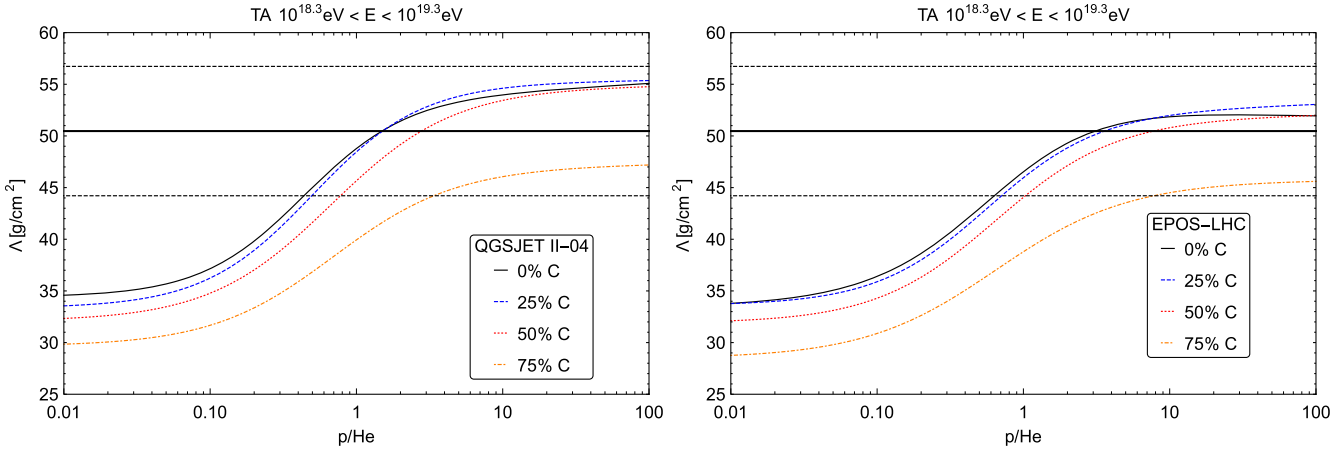

FIG. 4. Λ parameter as a function of proton-to-helium ratio for two-component mixture (p and He, black line) and three component mixtures (p, He and 25% C—green line; p, He and 50% C—red line; p, He and 75% C—orange line) of Monte-Carlo events simulated with QGSJET II-04 (left) and EPOS-LHC (right). Black solid and dashed lines correspond to the experimental value $\Lambda = 50.47 \pm 6.26$ g/cm^2 obtained by the Telescope Array collaboration [26].

as well based on the common assumption that the shower properties depend smoothly on $\ln A$.

IV. CONCLUSION

Let us finally discuss the possible applications of the obtained lower limit on the proton-to-helium ratio at the energies $10^{18.0}$ eV $< E < 10^{19.3}$ eV. First of all, we consider the properties of the sources of the ultrahigh-energy cosmic rays in the view of the constraints Eqs. (1) and (2). The present limits constrain the models with helium domination in the energy range under study, e.g., the helium version of the disappointing model [10]. These models generally include the preferential acceleration of helium or an excessive helium abundance at the acceleration region. The result of the present paper is fully compatible with the original pure proton dip model [7–9] as well as with the standard disappointing model [10] with $\mathrm{p/He} \sim 1$ while the modification of the dip model with $\mathrm{p/He} = 5$ [32] is disfavored by the Auger data Eq. (1).

Second, let us discuss the safety of the future colliders. The proof of the safety relies largely on the existence of non-zero flux of the ultrahigh-energy protons [15]. One may see from the Fig. 3 that expected Λ for models with zero proton flux is more than 5 standard deviation away from the value measured by the Pierre Auger Observatory. Hence the safe operation of the future colliders is supported at the high confidence level.

ACKNOWLEDGMENTS

We would like to thank L. Bezrukov, O. Kalashev, M. Kuznetsov, M. Pshirkov, A. Sokolov, and S. Troitsky for helpful comments and suggestions. The authors are indebted to the members of the Telescope Array collaboration for inspiring discussions. The present work is supported by the Russian Science Foundation Grant No. 17-72-20291. The numerical part of the work is performed at the cluster of the Theoretical Division of Institute for Nuclear Research of the Russian Academy of Sciences.

[1] R. Aloisio, V. Berezinsky, and P. Blasi, J. Cosmol. Astropart. Phys. 10 (2014) 020.
[2] G. Gelmini, O. E. Kalashev, and D. V. Semikoz, J. Exp. Theor. Phys. **106**, 1061 (2008).
[3] D. Hooper, A. M. Taylor, and S. Sarkar, Astropart. Phys. **34**, 340 (2011).
[4] V. S. Berezinsky and G. T. Zatsepin, Phys. Lett. **28B**, 423 (1969).
[5] K. Kotera, D. Allard, and A. V. Olinto, J. Cosmol. Astropart. Phys. 10 (2010) 013.
[6] T. Karg *et al.* (IceCube, Pierre Auger, and Telescope Array Collaborations), J. Phys. Soc. Jpn. Conf. Proc. **9**, 010021 (2016).
[7] V. Berezinsky, A. Z. Gazizov, and S. I. Grigorieva, Phys. Rev. D **74**, 043005 (2006).
[8] V. Berezinsky, A. Z. Gazizov, and S. I. Grigorieva, Phys. Lett. B **612**, 147 (2005).
[9] R. Aloisio, V. Berezinsky, P. Blasi, A. Gazizov, S. Grigorieva, and B. Hnatyk, Astropart. Phys. **27**, 76 (2007).
[10] R. Aloisio, V. Berezinsky, and A. Gazizov, Astropart. Phys. **34**, 620 (2011).
[11] K. Greisen, Phys. Rev. Lett. **16**, 748 (1966).
[12] Z. T. Zatsepin and V. A. Kuz'min, Zh. Eksp. Teor. Fiz. Pis'ma Red. **4**, 144 (1966).
[13] J. R. Ellis, G. Giudice, M. L. Mangano, I. Tkachev, and U. Wiedemann, J. Phys. G **35**, 115004 (2008).
[14] S. B. Giddings and M. L. Mangano, Phys. Rev. D **78**, 035009 (2008).
[15] A. V. Sokolov and M. S. Pshirkov, Eur. Phys. J. C **77**, 908 (2017).
[16] T. K. Gaisser *et al.* (HiRes Collaboration), Phys. Rev. D **47**, 1919 (1993).
[17] E. Barcikowski *et al.* (Pierre Auger and Yakutsk Collaborations), EPJ Web Conf. **53**, 01006 (2013).
[18] W. Hanlon *et al.*, J. Phys. Soc. Jpn. Conf. Proc. **19**, 011013 (2018).
[19] K. H. Kampert and M. Unger, Astropart. Phys. **35**, 660 (2012).
[20] J. Bellido *et al.* (Pierre Auger Collaboration), Proc. Sci. ICRC2017 (**2017**) 506 [arXiv:1708.06592].
[21] W. Hanlon *et al.*, Proc. Sci. ICRC2017 (**2017**) 536.
[22] R. U. Abbasi *et al.* (Telescope Array Collaboration), Astrophys. J. **858**, 76 (2018).
[23] S. Blaess, J. A. Bellido, and B. R. Dawson, arXiv:1803.02520 [Phys. Rev. D (to be published)].
[24] R. Ellsworth *et al.* (Fly's Eye Collaboration), Phys. Rev. D **26**, 336 (1982).
[25] R. M. Baltrusaitis, G. L. Cassiday, J. W. Elbert, P. R. Gerhardy, S. Ko, E. C. Loh, Y. Mizumoto, P. Sokolsky, and D. Steck (Fly's Eye Collaboration), Phys. Rev. Lett. **52**, 1380 (1984).
[26] R. U. Abbasi *et al.* (Telescope Array Collaboration), Phys. Rev. D **92**, 032007 (2015).
[27] P. Abreu *et al.* (Pierre Auger Collaboration), Phys. Rev. Lett. **109**, 062002 (2012).
[28] R. Ulrich, Proc. Sci. ICRC2015 (**2016**) 401.
[29] A. Yushkov, M. Risse, M. Werner, and J. Krieg, Astropart. Phys. **85**, 29 (2016).
[30] P. L. Biermann, T. K. Gaisser, and T. Stanev, Phys. Rev. D **51**, 3450 (1995).

[31] Y. Ohira and K. Ioka, Astrophys. J. Lett. **729**, L13 (2011).
[32] R. Aloisio and V. Berezinsky, arXiv:1703.08671.
[33] D. Heck *et al.*, Forschungszentrum Karlsruhe, Institut für Kernphysik Karlsruher (IKP) Report No. FZKA-6019, 1998.
[34] S. Ostapchenko, Nucl. Phys. B, Proc. Suppl. **151**, 143 (2006).
[35] S. Ostapchenko, Phys. Rev. D **83**, 014018 (2011).
[36] T. Pierog, I. Karpenko, J. M. Katzy, E. Yatsenko, and K. Werner, Phys. Rev. C **92**, 034906 (2015).
[37] F. Fenu *et al.* (Pierre Auger Collaboration), Proc. Sci. ICRC2017 (**2017**) 486 [arXiv:1708.06592].
[38] D. Ivanov, Proc. Sci. ICRC2015 (**2016**) 349.
[39] R. U. Abbasi *et al.*, Astropart. Phys. **64**, 49 (2015).